

Thickness and viscosity of organic thin films probed by combined surface acoustic Love wave and surface plasmon resonance

J.-M Friedt
FEMTO-ST, Dpt LPMO
32, avenue de l'Observatoire
25044 Besançon Cedex FRANCE

L. A. Francis
IMEC MCP/TOP
Kapeldreef 75
3001 Leuven BELGIUM

S. Ballandras
FEMTO-ST, Dpt LPMO
32, avenue de l'Observatoire
25044 Besançon Cedex FRANCE

Abstract—Direct detection biosensors aim at detecting molecular (antibody-antigen, DNA hybridation, cell attachment) binding events by means of electrical, mechanical or optical effects. A quantitative analysis of the amount of material bound to the surface requires the knowledge of the physical properties of the layer, namely optical index/dielectric constant, density, thickness, and a proper model of the interaction of this layer with the probing field (acoustic or optical). We here focus on the in-situ identification of the physical properties of thin organic (polymer and protein) layers bound to a substrate supporting the propagation of surface acoustic waves. In order to resolve some uncertainty on the resulting acoustic parameters, we propose the *simultaneous* probing of the same bound layer by optical methods (surface plasmon resonance) in a combined instrument as a means to uniquely identify the physical properties of the layer, namely the density, optical index, viscosity and thickness of the layer. We illustrate this technique for protein layers of collagen and fibrinogen. We then propose two models – transmission line and harmonic admittance computation – for analyzing these data and extract a quantitative viscosity information.

I. INTRODUCTION

Acoustic gravimetric sensors have been classically used for rigid mass detection, typically during cleanroom-type thin film vacuum deposition [1]. When extending these techniques to measurements in liquid media such as in the case of biosensors, it has been for long noticed that the frequency shift observed is not consistent through a simple proportionality factor with masses of molecules bound to the surface. These observations were made early in electrochemistry experiments in which current measurement provide an independent estimate of the deposited mass, and more recently in biochemical experiments [2]. An additional contribution to the gravimetric effect is the viscous interaction of the acoustic wave with the surrounding solvent. Depending on the characteristics of the layer (solvent concentration, roughness [3], [4], density, thickness, viscosity) the relative contribution of the viscous interaction to gravimetric might be predominant [5] or negligible. A proper analysis of the interaction of acoustic sensors requires a model including both contributions as well as relevant numerical constants to include in the models. Our purpose here is to tackle both aspects: fast and phenomenological transmission line model or slower but physically accurate

harmonic admittance computation for the modelling part, and an experimental part focusing on the combination of acoustic and optical methods in order to identify relevant physical parameters of the layer such as density and optical index both related to solvent content of the layer, thickness and viscosity of the layer. Other effects such as surface roughness are not included in these models.

II. EXPERIMENTAL SETUP

The experimental setup has been described in detail previously [6]. Basically, a Love mode acoustic wave sensor is made of a stack of 1.2 μm PECVD-deposited SiO_2 coated with 50 nm Au on an ST-quartz wafer. The acoustic wavelength is 40 μm : this value will be used in all models presented here. A liquid cell made of SU8 [7] confines the liquid to the gold-coated sensing area. The open well thus formed is filled with buffer solution for a baseline measurement, followed by protein mixed in this same buffer, and finally buffer for a final baseline measurement. During all these steps the coupling surface plasmon resonance (SPR) angle at a fixed wavelength of 670 nm is monitored (1 curve of reflected intensity vs. laser incidence angle in a 6° range per second), as well as the magnitude (insertion loss) and phase of the acoustic signal transmitted through the sensor is measured by a HP4396A network analyzer.

We observe (Fig. 1, top) a very large insertion loss increase during collagen (300 $\mu\text{g}/\text{ml}$) adsorption (-6.2 dB), hinting at the fact that the adsorbed layer strongly interacts with the surrounding solvent and hence dissipates acoustic energy. The SPR coupling angle shift is 723 m° and the phase shift of the acoustic sensor is -19.1 $^\circ$.

Fibrinogen (460 $\mu\text{g}/\text{ml}$) displays (Fig. 1, bottom) similar trends with an SPR coupling angle shift of 755 m° and the phase shift of the acoustic sensor of -13.2 $^\circ$ but a markedly lower insertion loss drop upon adsorption in the 0.7 ± 0.2 dB range, with a larger uncertainty range because of some drift of this quantity during this particular experiment.

These are the values we will attempt to fit in the models describing the physical properties of the adsorbed layer.

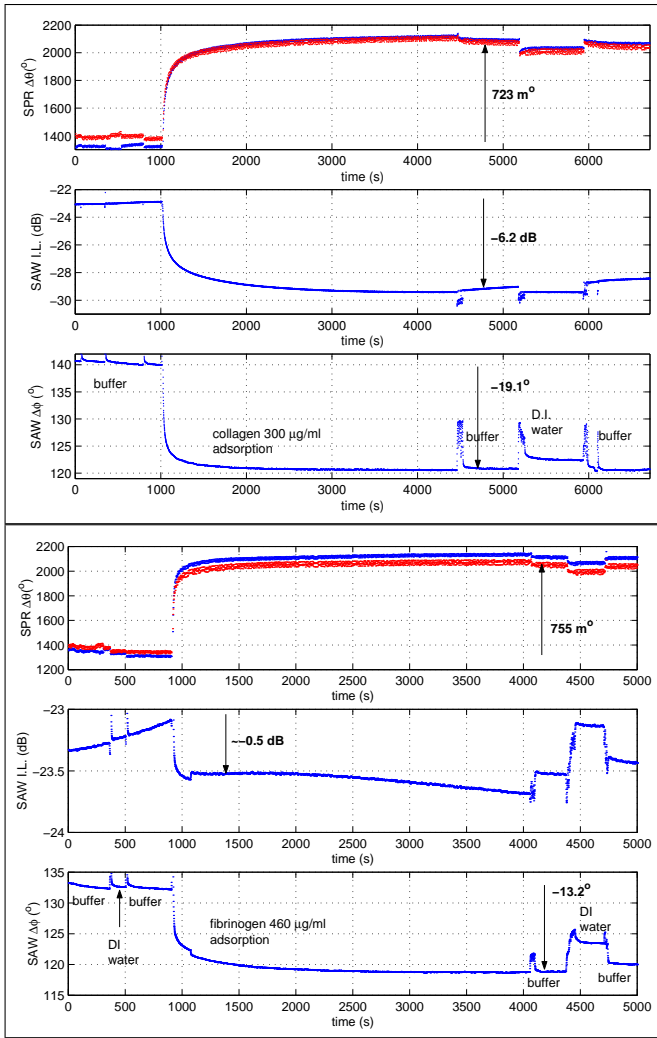


Fig. 1. Top: adsorption kinetics measurements of 300 $\mu\text{g/ml}$ collagen on hydrophobic thiol coated gold supporting simultaneously optical SPR (top) and acoustic Love-mode SAW (middle and bottom). Bottom: adsorption kinetics measurements of 460 $\mu\text{g/ml}$ fibrinogen on hydrophobic thiol coated gold with the same experimental setup.

One issue concerns the phase to frequency conversion: our openloop measurements monitor a phase variation at fixed frequency close to the maximum transmission frequency (as seen on a network analyzer). The transmission line model indeed computes at fixed frequency the phase variation as a function of the adsorbed layer material properties (thickness, density, viscosity). On the other hand the mixed-matrix model computes a full transfer function of the stack of layers and from these we deduce a frequency shift (as computed by searching the position of the maximum of the modulus of the transfer function) and the insertion loss per wavelength is deduced – considering that the relaxation time of a resonator of quality factor Q is $\frac{Q}{\pi}$ periods – through

$$\text{IL}/\lambda = 20 \times \log_{10}(e) \times \pi/Q$$

However the frequency shift is to be converted to a phase shift for comparison with the transmission line model and the exper-

imental results. Experimentally we observed a linear phase to frequency slope $\frac{d\varphi}{df}$ of $0.593 \times 10^{-3} \text{ }^\circ/\text{Hz}$, which is consistent with the expected value of $\frac{d\varphi}{df} = 2\pi \frac{L}{V} = 0.576 \times 10^{-3} \text{ }^\circ/\text{Hz}$ where $V = \lambda f \simeq 4740 \text{ m/s}$ is the acoustic wave group velocity (close to the phase velocity here) and $L = 8 \text{ mm}$ the center to center distance between the interdigitated transducers. In our comparisons between model and experiment we used the experimental value to convert from phase to frequency shifts.

III. MODELS

Two models have been developed to fit acoustic experiments to possible physical parameters of the layers adsorbed on the surface: a transmission line model and a harmonic admittance computation based on the Blötekjær approach. The latter model has been described in detail in [8].

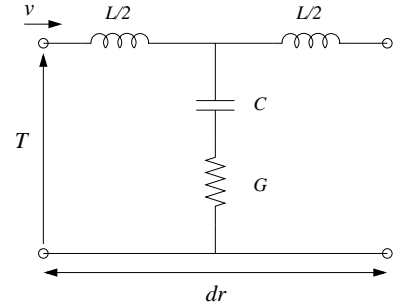


Fig. 2. Differential element of the viscoelastic mechanical transmission line model: the shear stress (T) and the shear wave particle velocity (v) propagate through a symmetric differential element of length dr made of an inductance L (equivalent density ρ of the layer) shunted by the series connection of a capacitance C (shear stiffness of the layer) and a conductance G (shear viscosity of the layer).

The former model is based on an equivalent transmission line model including a viscous interaction component in the form of a shunt capacitance $C = \frac{1}{\mu}$, μ being the shear stiffness, placed in series with a conductance $G = \frac{1}{\eta}$, η being the dynamic viscosity, as shown in Fig. 2. The bound mass component is included as the inductor $L = \rho$ with ρ the density of the layer.

The latter – specifically developed to address the problem of modelling damping effects of Surface Acoustic Waves (SAW) by an ideal newtonian fluid – is based on a Fahmy-Adler eigenvalue representation of the elastic propagation problem. This calculation has been extended to include viscous interactions through a stress T_{ij} to strain S_{ij} relationship written as

$$T_{ij} = - \left(P + j\omega \left(\frac{2}{3}\eta - \zeta \right) S_{kk} \right) \delta_{ij} + 2\omega\eta S_{ij}$$

where ω is the angular frequency, P is the fluid pressure proportional to the displacement divergence via the fluid compressibility χ : $P = -\frac{\partial u_i}{\chi \partial x_i}$, ζ is the compressive viscosity and η the shear (absolute) viscosity. We have verified that in the case of Love mode (which are purely shear waves) the compressional viscosity does not affect the result: we will always take the tabulated value for water $\zeta = 2.8 \text{ cP}$.

In both cases we use the same material parameters for modelling the propagation of a Love mode surface acoustic wave on ST-cut quartz coated with $1.2 \mu\text{m}$ SiO_2 and 50 nm Au . We have used the somewhat unusual $c_{44} = c_{55} = c_{66} = 8.31 \text{ GPa}$ coefficient as experimentally deduced from the dispersion curve experimentally observed during wet etching of the silicon dioxide guiding layer by hydrofluoric acid [9]. This difference between material properties observed for our thin film compared to tabulated values for bulk material is not unusual though [10].

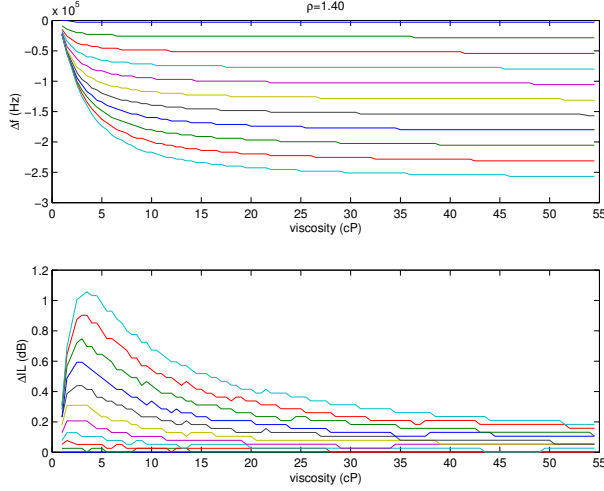


Fig. 3. Insertion loss and resonance frequency shifts upon thin film adsorption on a stack made of ST-quartz (substrate) coated with $1.2 \mu\text{m}$ PECVD- SiO_2 , 50 nm Au , the whole simulation being performed with an infinite top-most medium of water. The parameters under investigation are the thickness, density and viscosity of the adsorbed thin (protein) film. Top: the parameter in abscissa is the viscosity, while the successive curves display increasing layer thicknesses from 0 to 50 nm by steps of 5 nm , the density of the layers being kept constant at $\rho = 1.4 \text{ g/cm}^3$. For comparison, the viscosity of pure water is 1 cP while water mixed with glycerin (80% weight to weight) leads to a solution with viscosity 60 cP at $20 \text{ }^\circ\text{C}$.

Figs. 3 and 4 display the variation of resonance frequency and insertion loss for our geometry (a sensing length of $4.9 \text{ mm} = 122.5\lambda$): as would be expected, the evanescent shear acoustic wave at frequency $f \simeq 118.5 \text{ MHz}$ probes only to a few skin depths $\delta = \sqrt{\frac{\eta}{\pi \rho f}} = 52 \text{ nm}$. A more surprising result is the enhancement of the signal, both as a frequency shift and damping enhancement when the thickness reaches values in the $50\text{-}70 \text{ nm}$ range depending on the viscosity. Similarly, for a given thickness, the damping signal is strongly enhanced for shear viscosities in the 3 to 5 cP range and mostly independent of the density of the layer.

In parallel to these acoustic models, an optical model providing the reflection coefficient of a stack of planar layers as a function of coupling angle at a given wavelength has been used to predict the SPR angle shift as a function of layer thickness and optical index (Fig. 5). We have assumed here that the optical index is a weighted function of the protein to solvent fraction $x \in [0 : 1]$. Here again for large layer thicknesses, the evanescent optical wave is no longer able to probe the change in dielectric constant during adsorption and

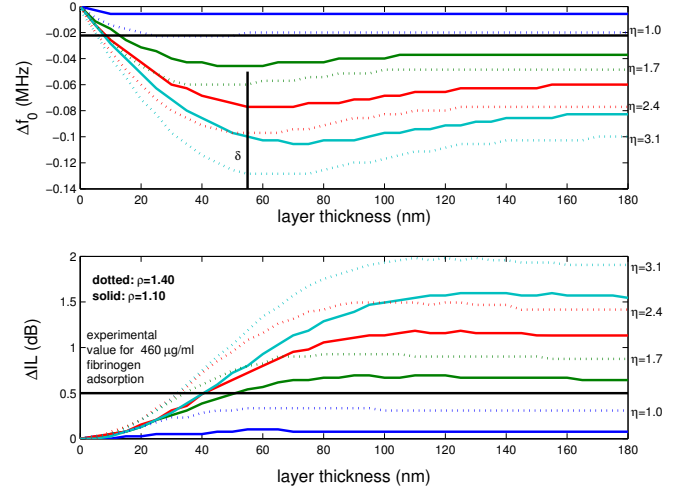


Fig. 4. Simulation with the same parameters as those of Fig. 3, with this time the parameter in abscissa being the thickness analyzed a on wide range to reach the penetration depth δ of the shear wave in liquid (depth probed by the acoustic sensor) while the various curves display viscosity variations from 1 to 3.1 cP by steps of 0.7 cP . Dotted lines are for a layer density of 1.40 (mostly protein), solid lines for a layer density of 1.10 (mostly solvent). The thick horizontal lines at $\Delta f_0 = 0.022 \text{ MHz}$ and $\Delta IL = 0.5 \text{ dB}$ indicate the experimental values observed during fibrinogen adsorption on hydrophobic thiols.

the signal saturates.

IV. RESULTS AND DISCUSSION

We have observed the adsorption kinetics of various kinds of proteins selected for their expected different mechanical behaviors. Our previous studies focused on globular proteins [6], [11] which were expected to behave as mostly rigid layers containing only a small proportion of solvent within a compact stack of proteins adsorbed on a surface. On the other hand fibrinogen and collagen are fibrous proteins with elongated structure which display a geometry consistent with layers strongly interacting with the surrounding solvent and hence expected to display significant viscous contribution. Indeed, raw acoustic results strongly hint at such a behavior: quartz-crystal microbalance with dissipation measurements [2] indicate strong dissipation increase upon protein adsorption on hydrophobic-thiol coated gold surfaces, while the insertion loss of surface acoustic wave sensors display an important variation.

We now include in these new models, in addition to the classically used gravimetric interaction,

- as a new variable the viscosity of the adsorbed layer and hence a new component in the model
- as a new measured quantity the insertion of the surface acoustic wave sensor.

We identify the ratio of the insertion loss variation during the experiment (from baseline before adsorption to baseline after adsorption of a biochemical layer, both measurements being made in the same reference buffer) to the phase shift variation as a relevant estimate of the relative contributions of viscous to gravimetric effects.

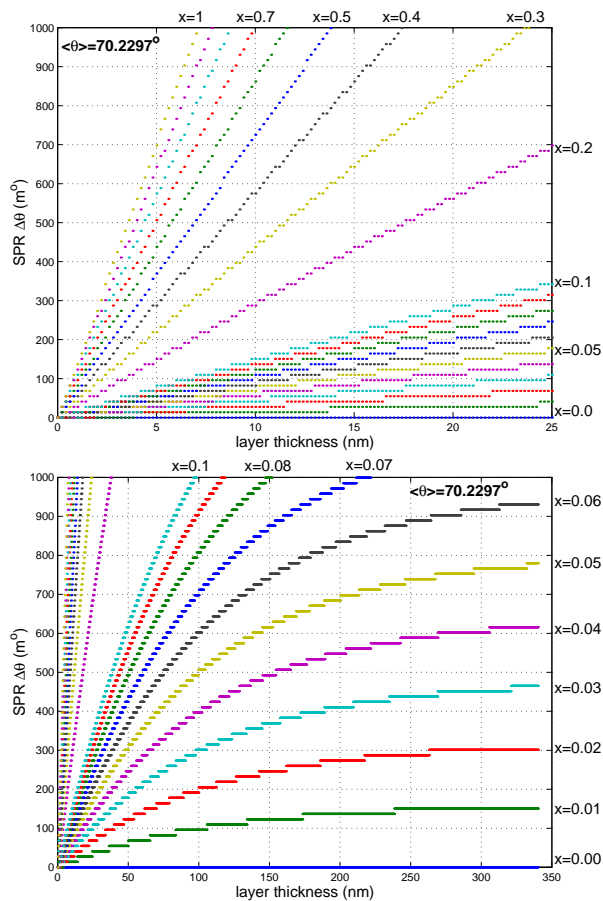


Fig. 5. Top: simulation of the SPR dip minimum position as a function of protein to solvent fraction (x) meaning the optical index n varies from 1.33 (pure water) to 1.45 (pure protein layer) as $n = x \times 1.45 + (1 - x) \times 1.33$. For thin layers the SPR dip position shifts linearly with the thickness of the layer. Bottom: same simulation for a thicker layer: we see here the penetration depth of the evanescent optical field leading to a decreasing angle shift with increasing thickness. Only very diluted layers ($x \in [0 : 0.1]$) can lead to SPR angle shifts compatible with experimental measurements for such a thick layer.

However, within reasonable density ranges ($\rho \in [1 : 1.45]$) for the protein layer and for all possible viscosity values analyzed here, the Newtonian fluid interaction with the shear acoustic wave is unable to fit experimental data of insertion loss variations during collagen adsorption ($\Delta IL > 2$). We thus conclude that a simple Newtonian fluid model is insufficient to accurately represent the behavior of the biological layer probed by the acoustic sensor and that an extension to the Maxwellian fluid representation is needed, possibly including additional relaxation, non-linear and delayed effects. This implementation is much more difficult than that of the Newtonian fluid since the delayed relaxation of the fluid interacting with the acoustic wave leads to non-linear terms and is hence unsuitable for a transmission line model.

V. CONCLUSION

We have presented experimental results based on combined acoustic and optical methods monitoring the adsorption kinetics of collagen and fibrinogen on hydrophobic thiols.

In order to interpret the resulting data and extract relevant physical quantities characteristic of these layers – viscosity, layer thickness, density and optical index – we have developed two models including viscoelasticity as Newtonian fluid interactions.

Interestingly, we can conclude from these models:

- there exists a low viscosity range for which the insertion loss strongly amplifies the transduction signal,
- the ΔIL and $\Delta\varphi$ signals saturate for layer thicknesses beyond 150 nm, consistent with the propagation depth of the evanescent shear acoustic wave for a working frequency around 125 MHz.

However, these models are insufficient to interpret all data and specifically the very large insertion loss increase (> 2 dB) upon adsorption of these very viscous layers.

ACKNOWLEDGMENT

L. A. Francis thanks the Belgian FRIA (Fonds pour la Formation à la Recherche dans l'Industrie et dans l'Agriculture) for financial support. We acknowledge the help of R. Giust (FEMTO-ST/LOPMD, Besançon, France) for kindly providing the SPR simulation software.

REFERENCES

- [1] A. Janshoff, H. J. Galla, and C. Steinem, "Piezoelectric mass sensing devices as biosensors – an alternative to optical biosensors?" *Angew. Chem. Int. Ed. Engl.*, vol. 39, pp. 4004–4032, 2000.
- [2] M. Rodahl, F. Höök, C. Fredriksson, C. A. Keller, A. Krozer, P. Brzezinski, M. Voinova, and B. Kasemo, "Simultaneous frequency and dissipation factor qcm measurements of biomolecular adsorption and cell adhesion," *Faraday Discussions*, vol. 107, pp. 229–246, 1997.
- [3] M. Urbakh, L. Daikhin, and J. Klafter, "Dynamics of confined liquids under shear," *Phys. Rev. E*, vol. 51, no. 3, pp. 2137–2141, 1995.
- [4] L. Daikhin, E. Gileadi, G. Katz, V. Tsionsky, M. Urbakh, and D. Zsigmond, "Influence of roughness on the admittance of the quartz crystal microbalance immersed in liquids," *Anal. Chem.*, vol. 74, pp. 554–561, 2002.
- [5] K. Saha, F. Bender, A. Rasmussen, and E. Gizeli, "Probing the viscoelasticity and mass of a surface-bound protein layer with an acoustic waveguide device," *Langmuir*, vol. 19, no. 4, pp. 1304–1311, 2003.
- [6] J.-M. Friedt, L. Francis, G. Reekmans, R. D. Palma, A. Campitelli, and U. Sleytr, "Simultaneous surface acoustic wave and surface plasmon resonance measurements: electrodeposition and biological interactions monitoring," *J. Appl. Phys.*, vol. 95, no. 4, pp. 1677–1680, 2004.
- [7] L. Francis, J.-M. Friedt, C. Bartic, and A. Campitelli, "A SU8 liquid cell for surface acoustic waves biosensors," *Proceedings of SPIE*, vol. 5455, pp. 353–363, 2004.
- [8] S. Ballandras, A. Reinhardt, A. Khelif, M. Wilm, V. Laude, W. Daniau, and V. Blondeau-Pâtissier, "Theoretical analysis of damping effects of guided elastic waves at solid/fluid interfaces," *J. Appl. Phys.*, 2005, submitted.
- [9] L. Francis, J.-M. Friedt, R. de Palma, C. Zhou, C. Bartic, P. Bertrand, and A. Campitelli, "Techniques to evaluate the mass sensitivity of love mode surface acoustic wave biosensors," in *IEEE International Ultrasonics Conference*, 2004, pp. 241–249.
- [10] C. Zimmermann, P. Mazein, D. Rebière, C. Dejous, F. Josse, and J. Pistré, "A theoretical study of love wave sensors mass loading and viscoelastic sensitivity in gas and liquid environments," in *IEEE International Ultrasonics Conference*, 2004, pp. 813–816.
- [11] C. Zhou, J.-M. Friedt, A. Angelova, K.-H. Choi, W. Laureyn, F. Frederix, L. A. Francis, A. Campitelli, Y. Engelborghs, and G. Borghs, "Human immunoglobulin adsorption investigated by means of quartz crystal microbalance dissipation, atomic force microscopy, surface acoustic wave, and surface plasmon resonance techniques," *Langmuir*, vol. 20, no. 14, pp. 5870–5878, 2004.